Astron. Astrophys. 362, 978–983 (2000)

ASTRONOMY
AND
ASTROPHYSICS

Polarization measurements of Vega-like stars

H.C. Bhatt and P. Manoj

Indian Institute of Astrophysics, Bangalore 560 034, India (hcbhatt,manoj@iiap.ernet.in)

Received 6 June 2000 / Accepted 8 September 2000

Abstract. Optical linear polarization measurements are presented for about 30 Vega-like stars. These are then compared with the polarization observed for normal field stars. A significant fraction of the Vega-like stars are found to show polarization much in excess of that expected to be due to interstellar matter along the line of sight to the star. The excess polarization must be intrinsic to the star, caused by circumstellar scattering material that is distributed in a flattened disk. A correlation between infrared excess and optical polarization is found for the Vega-like stars.

Key words: polarization – stars: circumstellar matter – infrared: stars

1. Introduction

The Infrared Astronomy Satellite (IRAS) detected (Aumann et al. 1984) a large infrared excess at wavelengths longward of $12\,\mu$ from the otherwise normal main-sequence A0V star Vega (α Lyr). The infrared excess is thought to be due to emission from circumstellar dust, in thermal equilibrium with the stellar radiation from the central star, and distributed in a shell or ring, several tens to hundred AU in extent. Since then a large number of main-sequence stars have been found to have similar infrared excesses in the IRAS wavebands and are called Vega-like stars (see eg. Backman & Paresce 1993, Vidal-Madjar & Ferlet 1994, Lagrange-Henri 1995, Mannings & Barlow 1998).

What is the spatial distribution of the circumstellar dust in Vega-like stars? Optical coronagraphic observations of β Pic by Smith & Terrile (1984) showed that the scattering dust in this object is distributed in a flattened disk being viewed nearly edge-on. Vega-like stars are now generally thought to have circumstellar dust distributed in disks. The disk structures in these objects may be the end products of evolution of more massive disks associated with pre-main-sequence stars and are replenished by the dust debris produced by the disruption of planetesimals due to collisional and thermal evaporation processes (eg. Backman & Paresce 1993, Malfait et al. 1998). However, other than for β Pic, direct evidence for the flattened disk-like distribution of the circumstellar material around Vega-like stars has so far been obtained only for a handful of these objects by optical and infrared imaging (BD +31°643, Kalas & Jewitt 1997; SAO 26804, Skinner et al. 1995; HR 4796A, Jayawardhana et al. 1998 and Koerner et al. 1998).

Circumstellar dust emits thermally in the infrared producing the infrared excess. It also scatters the stellar radiation giving rise to reflection nebulosity. Another manifestation of scattering by dust in the circumstellar disk can be polarization of the stellar radiation. For example, the polarization observed in the light of young T Tauri stars and the Herbig Ae/Be stars is generally ascribed to dusty circumstellar disks (e.g. Bastien 1988). Therefore, it is of interest to look for polarization in Vega-like stars. In β Pic, where the disk can be resolved, imaging polarimetry in the R band shows linear polarization at the level of $\sim 17\%$ (Gledhill et al. 1991). When the disk cannot be resolved, any polarization in the integrated light from the *star + disk* system will show much lower values of polarization depending on the amount of scattering dust, degree of flattening of the disk and its orientation with respect to the observer's line of sight to the star. In the observed polarization for an object, there will also be present a component of the interstellar polarization that will depend on the direction and distance to the star. Any significant intrinsic component of polarization in the observed polarization for a star will indicate the presence of circumstellar dust with a spatial distribution around the star that is not spherically symmetric. The dust could be in a disk-like structure with the disk-plane making relatively small angles with the line of sight, because a circularly symmetric disk at right angles to the line of sight will produce no net polarization in the integrated light. Thus polarization measurements can give important information on the spatial distribution of scattering dust in Vega-like stars.

In this paper we present the results of optical linear polarization measurements of about 30 Vega-like stars. We also compile polarization data on additional Vega-like stars from the literature. The Vega-like stars are then compared with normal field stars. It is found that a significant fraction of the Vega-like stars show polarization that is much larger than can be explained as due to the interstellar polarization. In Sect. 2 we present our measurements. Comparison with field stars, the intinsic polarization of Vega-like stars, the distribution and nature of the dust grains is discussed in Sect. 3. The conclusions are summarized in Sect. 4.

Send offprint requests to: H.C. Bhatt

Table 1. Polarization measurements of Vega-like stars

HD number	Date of Observation (1999)	Spectral Type	V mag	B-V mag	E(B-V) mag	m-M	Ref	P(%)	ϵ_P(%)	$\theta(^\circ)$	$\epsilon_\theta(^\circ)$
9672	17Jan	A1V	5.6	0.06	0.04	3.94	H	0.17	0.05	12	8
17206	17Jan	F5/F6V	4.4	0.48	0.03	0.73	H	0.10	0.03	88	5
17443	17Jan	B9V	8.7	0.30	0.38	7.67	H	1.10	0.17	139	5
32509	16Jan	A2	7.5	0.20	0.15	5.89	H	0.95	0.09	51	3
34700	17Jan	G0	9.1	0.56	0.00	10.32	H	0.11	0.12	37	19
37389	17Jan	A0	8.3	-0.06	0.00	7.04		0.46	0.12	15	8
53300	16Jan	A0	8.0	0.31	0.31	5.79		1.00	0.13	81	3
93331	08Apr	B9.5V	7.2	0.02	0.07	5.90	H	0.24	0.06	175	5
98800	13Mar	K5	8.8	1.15	0.10	3.34	H	0.54	0.13	89	6
99211	08Apr	A9V	4.0	0.21	0.00	2.05	H	0.06	0.06	175	5
102647	07Apr	A3V	2.1	0.09	0.01	0.22	H	0.15	0.05	50	6
109085	08May	F2V	4.3	0.38	0.03	1.30	H	0.38	0.04	147	5
115892	08Apr	A2V	2.7	0.06	0.18	1.27	H	0.18	0.06	164	6
121847	08May	B8V	5.2	-0.08	0.01	5.09	H	0.53	0.04	172	2
123247	08May	B9V	6.4	0.00	0.07	5.02	H	0.21	0.06	57	5
131885	08Apr	A0V	6.9	0.01	0.01	5.42	H	0.57	0.07	13	3
135344	11Mar	A0V	8.6	0.48	0.48	5.82		0.07	0.11	108	15
139614	10Mar	A7V	8.2	0.23	0.03	5.76		0.65	0.10	38	5
139664	12Mar	F5IV/V	4.6	0.41	0.00	1.22	H	0.76	0.07	165	5
142096	06may	B3V	5.0	-0.01	0.18	5.19	H	0.42	0.04	173	2
142114	08May	B2.5V	4.5	-0.07	0.15	5.62	H	0.45	0.05	14	2
142165	06May	B5V	5.3	-0.01	0.15	5.52	H	0.75	0.06	3	2
142666	11Mar	A8V	8.8	0.52	0.27	5.51		0.80	0.12	72	4
143006	08Apr	G6/G8	10.2	0.73	0.03	4.82		0.69	0.08	7	3
145482	08may	B2V	4.5	-0.17	0.06	5.78	H	0.50	0.05	117	4
149914	11Mar	B9.5IV	6.7	0.24	0.29	6.09	H	2.54	0.07	66	1
233517	10Mar	K2	9.7	1.30	0.40	2.16		1.80	0.21	177	4

H in the Ref. column refers to the*Hipparcos* catalogue

2. Observations

Optical linear polarization measurements were made with a fast star-and-sky chopping polarimeter (Jain & Srinivasulu 1991) coupled at the $f/13$ Cassegrain focus of the 1-m telescope at the Vainu Bappu Observatory, Kavalur of the Indian Institute of Astrophysics. A dry-ice cooled R943-02 Hamamatsu photomultiplier tube was used as the detector. All measurements were made in the V band with an aperture of 15 *arcsec*. Observations were made during the period of January to May 1999. The instrumental polarization was determined by observing unpolarized standard stars from Serkowski (1974). It was found to be $\sim 0.1\%$, and has been subtracted vectorially from the observed polarization of the programme stars. The zero of the polarization position angle was determined by observing the polarized standard stars from Hsu & Breger (1982). The position angle is measured from the celestial north, increasing eastward. The Vega-like stars selected for observations were taken from the lists of Vega-like objects in Backman & Paresce (1993), Coulson et al. (1996) and Mannings & Barlow (1998).

The results of our polarization measurements are presented in Table 1. We observed 27 Vega-like stars. In Table 1, the HD numbers of the stars observed are given in Column 1, the date of observation in Column 2, spectral type in Column 3, V magnitude in Column 4, the colour $B-V$ in Column 5, colour excess $E(B-V)$ in Column 6 and the distance modulus $m-M$ in Column 7. For most of the stars the stellar parameters and the the distance modulus are taken from the $Hipparcos$ catalogue (ESA 1997) as indicated by H in the reference Column 8. Stars for which $Hipparcos$ distances are not available, the distance modulus is estimated from spectral type and photometric magnitudes. Intrinsic colours and absolute magnitudes are taken from Schmidt-Kaler (1965). The distance modulus has been corrected for extinction by using a value of 3.0 for the ratio of total to selective extinction $A_V/E(B-V)$. The extinction values are generally quite small. Negative values of $E(B-V)$ in Column 6 have been called zero to derive the corrected magnitudes of the stars. The observed degree of polarization $P(\%)$ and the position angle $\theta(^\circ)$ are given in Columns 9 and 11, while the probable errors in the measurements of polarization ϵ_P and the position angle ϵ_θ are given in Columns 10 and 12.

3. Discussion

It can be seen from Table 1 that the degree of polarization for the Vega-like stars varies from small values of $\sim 0.06\%$ (for HD 99211) to values as large as $\sim 2.5\%$ (for HD 149914). Most of the Vega-like stars are nearby objects within $\sim$ 100 *pc*

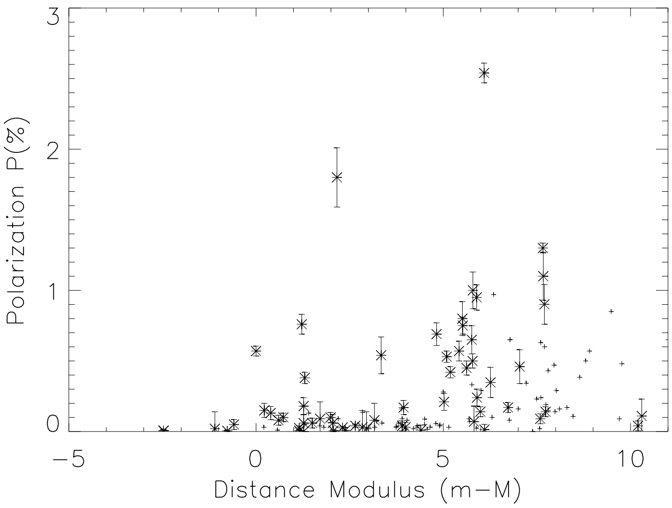

Fig. 1. Percentage polarization plotted against distance modulus for Vega-like stars. Vega-like stars are represented by the asterix symbol while crosses are used for normal stars

and are at large galactic latitudes ($|b|$ generally $> 10°$, due to a selection effect in making the searches for stars with excess far-infrared fluxes in the IRAS catalogue). At such short distances the contribution of the interstellar polarization to the observed polarization is expected to be small $\sim 0.1\%$. A significant fraction (about 2/3) of the Vega-like stars have polarization values $> 0.3\%$. As discussed below, such large values indicate intrinsic polarization being caused by the circumstellar dust around the Vega-like stars.

As most of the known Vega-like stars are relatively bright objects, a number of them are likely to have been observed earlier as part of other polarimetric programmes. Therefore, to supplement our observations, we have made a search for polarization measurements of additional Vega-like stars in the $SIMBAD$ data base at CDS, Strasbourg. We found polarization measurements for 34 such stars in the catalogue of stellar polarization by Heiles (2000). In a manner similar to Table 1, we list data for these stars from Heiles (2000) in Table 2. Altogether, in Tables 1 and 2, we now have 61 Vega-like stars with polarization measurements. In the following we compare the polarimetric behaviour of the Vega-like stars with normal field stars.

In order to assess the strength of the intrinsic component in the polarization of the Vega-like stars, one needs to have an estimate of the interstellar polarization. For more distant Vega-like stars the interstellar component could be relatively large, since the interstellar polarization in general increases with distance, and should be subtracted from the observed polarization. This is, however, not possible for the programme stars individually, as the interstellar polarization in the direction of these stars, as a function of distance, is generally not known. We therefore make a statistical comparison between the polarization observed for the Vega-like stars and normal field stars with similar magnitudes and distances. For the comparison, polarization measurements for normal field stars have been taken from Heiles (2000). Normal stars within $\sim 1°$ of the Vega-like stars were chosen for comparison. Stars with any known peculiarities (like the presence of emission lines in the spectra, infrared excesses, association with nebulosities,variability etc.) were excluded. In Fig. 1 we plot the observed degree of polarization against the distance modulus for the Vega-like stars as well as the normal field stars. It can be seen from Fig. 1 that, on an average, the Vega-like stars have polarization values generally larger than the normal field stars at comparable distances. The average value of polarization for the Vega-like stars is 0.34% with a large dispersion of 0.48%, while the normal field stars have an average polarization of 0.2% and a smaller dispersion of 0.22%. Fig. 2 shows frequency distribution (as a fraction of the total number of stars in the two samples seperately) of stars with observed polarization larger than a given value. Now the difference between the polarimetric behaviour of the two samples of stars is more clear. About 30% of the Vega-like stars show polarization values larger than 0.5%, whereas only 13% of the normal field stars show polarization values larger than 0.5%. There are no field stars with polarization values larger than 1%, while about 10% of the Vega-like stars show polarization values larger than 1%. For the stars plotted in Fig. 1 a two-sided two-dimensional

Table 2. Polarization data for additional Vega-like stars from literature

HD Number	P(%)	ϵ_P(%)	$\theta(°)$	$\epsilon_\theta(°)$	E(B-V) mag	V mag	Spectral Type	m-M
3003	0.028	0.009	127.7	9.1	0.00	5.2	A2	2.31
10476	0.050	0.035	178.1	19.3	0.00	5.2	K1V	-0.59
10647	0.040	0.035	20.7	23.6	0.00	5.6	G0I	10.20
10700	0.005	0.007	148.9	35.0	0.00	3.6	G8V	-2.47
14055	0.030	0.120	18.0	63.4	0.00	4.0	A0V	2.84
16157	0.131	0.047	170.6	10.2	0.00	8.6	K7V	0.39
18978	0.006	0.006	10.8	26.6	0.00	4.2	A3V	2.07
20010	0.006	0.009	115.3	36.9	0.00	4.0	F8IV	1.15
22049	0.007	0.010	147.6	35.5	0.00	3.7	K2V	-2.47
38393	0.570	0.035	42.5	1.8	0.00	3.6	F6V	0.00
43955	0.090	0.035	63.1	11.0	0.10	5.3	B2V	7.59
49336	1.300	0.035	2.0	0.8	0.10	6.2	B3V	7.66
53376	0.014	0.037	175.5	54.0	0.01	9.3	F3/F5V	6.10
68456	0.060	0.035	166.4	16.3	0.00	4.8	F7V	1.50
69830	0.080	0.035	140.6	12.3	0.00	6.0	G8V	0.60
71155	0.020	0.120	13.0	71.6	0.00	3.9	A0V	2.95
73390	0.170	0.035	119.5	5.9	0.10	5.3	B3V	6.73
95418	0.000	0.120	43.0	90.0	0.00	2.4	A1V	1.27
108483	0.140	0.035	59.5	7.1	0.00	3.9	B2V	5.99
114981	0.140	0.035	32.3	7.1	0.10	7.1	B7	7.73
128167	0.090	0.120	26.0	33.7	0.00	4.5	F2	1.71
139006	0.060	0.120	29.0	45.0	0.00	2.2	A0V	1.27
143018	0.348	0.107	37.2	8.7	0.10	2.9	B1V	6.26
149630	0.080	0.120	75.0	36.9	0.10	4.3	B9V	3.16
153968	0.901	0.141	33.2	4.5	0.08	9.3	F0V	7.70
161868	0.008	0.001	33.3	3.6	0.10	3.8	A0V	2.38
162917	0.100	0.035	65.2	9.9	0.00	5.7	F4V	1.99
172167	0.020	0.120	75.0	71.6	0.00	0.0	A0V	-1.10
176638	0.030	0.035	13.5	30.3	0.00	4.7	A0V	3.99
181296	0.040	0.035	99.9	23.6	0.00	5.0	A0V	3.90
181869	0.010	0.035	75.9	60.3	0.00	4.0	B9II	4.40
214953	0.025	0.015	115.3	16.7	0.00	6.3	G0V	1.15
216956	0.005	0.005	122.9	26.6	0.00	1.3	A3V	-0.77
224392	0.041	0.011	128.5	7.6	0.00	5.2	A2V	2.65

Table 3. Estimated fractional infrared excesses (L_{IR}/L_*) for Vega-like stars

HD Number	(IRAS F_{12} (Jy)	Flux F_{25} (Jy)	Densities) F_{60} (Jy)	F_{100} (Jy)	L_{IR}/L_*
9672	3.31×10^{-01}	4.06×10^{-01}	$2.00 \times 10^{+00}$	$1.91 \times 10^{+00}$	1.64×10^{-3}
17206	$1.88 \times 10^{+00}$	6.54×10^{-01}	$1.63 \times 10^{+00}$	$5.01 \times 10^{+00}$	1.67×10^{-3}
17443	4.19×10^{-01}	$2.39 \times 10^{+00}$	$1.45 \times 10^{+01}$	$2.28 \times 10^{+01}$	6.32×10^{-2}
32509	4.33×10^{-01}	6.87×10^{-01}	$2.48 \times 10^{+00}$	$6.59 \times 10^{+00}$	1.22×10^{-2}
34700	6.05×10^{-01}	$4.42 \times 10^{+00}$	$1.41 \times 10^{+01}$	$9.38 \times 10^{+00}$	3.48×10^{-1}
37389	3.84×10^{-01}	$1.40 \times 10^{+00}$	$1.33 \times 10^{+01}$	$4.21 \times 10^{+01}$	1.65×10^{-1}
53300	7.48×10^{-01}	3.15×10^{-01}	4.14×10^{-01}	$2.80 \times 10^{+00}$	6.75×10^{-3}
93331	2.50×10^{-01}	2.54×10^{-01}	6.71×10^{-01}	$1.32 \times 10^{+00}$	3.38×10^{-3}
98800	$1.98 \times 10^{+00}$	$9.28 \times 10^{+00}$	$7.28 \times 10^{+00}$	$4.46 \times 10^{+00}$	1.63×10^{-1}
99211	$1.57 \times 10^{+00}$	4.27×10^{-01}	4.00×10^{-01}	$1.00 \times 10^{+00}$	7.34×10^{-4}
102647	$6.97 \times 10^{+00}$	$2.11 \times 10^{+00}$	$1.18 \times 10^{+00}$	$1.00 \times 10^{+00}$	4.56×10^{-4}
109085	$2.18 \times 10^{+00}$	7.73×10^{-01}	5.44×10^{-01}	$1.00 \times 10^{+00}$	1.18×10^{-3}
115892	$3.56 \times 10^{+00}$	9.72×10^{-01}	4.00×10^{-01}	$1.00 \times 10^{+00}$	2.44×10^{-4}
121847	2.39×10^{-01}	3.62×10^{-01}	$1.08 \times 10^{+00}$	$2.16 \times 10^{+00}$	7.06×10^{-4}
123247	1.33×10^{-01}	1.56×10^{-01}	5.13×10^{-01}	$4.40 \times 10^{+00}$	1.80×10^{-3}
131885	1.06×10^{-01}	2.14×10^{-01}	3.52×10^{-01}	$1.07 \times 10^{+00}$	1.84×10^{-3}
135344	$1.59 \times 10^{+00}$	$6.71 \times 10^{+00}$	$2.56 \times 10^{+01}$	$2.57 \times 10^{+01}$	8.38×10^{-2}
139614	$4.11 \times 10^{+00}$	$1.81 \times 10^{+01}$	$1.93 \times 10^{+01}$	$1.39 \times 10^{+01}$	3.41×10^{-1}
139664	$1.42 \times 10^{+00}$	6.93×10^{-01}	6.61×10^{-01}	$2.37 \times 10^{+00}$	1.44×10^{-3}
142096	5.55×10^{-01}	3.89×10^{-01}	6.46×10^{-01}	$1.30 \times 10^{+00}$	1.55×10^{-4}
142114	6.64×10^{-01}	$1.73 \times 10^{+00}$	$4.20 \times 10^{+00}$	$1.16 \times 10^{+01}$	4.02×10^{-4}
142165	2.50×10^{-01}	3.40×10^{-01}	$2.77 \times 10^{+00}$	$1.16 \times 10^{+01}$	9.01×10^{-4}
142666	$8.57 \times 10^{+00}$	$1.12 \times 10^{+01}$	$7.23 \times 10^{+00}$	$5.46 \times 10^{+00}$	2.32×10^{-1}
143006	8.57×10^{-01}	$3.16 \times 10^{+00}$	$6.57 \times 10^{+00}$	$4.82 \times 10^{+00}$	4.80×10^{-1}
145482	6.58×10^{-01}	$1.04 \times 10^{+00}$	$3.13 \times 10^{+00}$	$1.11 \times 10^{+01}$	3.78×10^{-4}
149914	3.90×10^{-01}	5.25×10^{-01}	$3.53 \times 10^{+00}$	$1.23 \times 10^{+01}$	4.77×10^{-3}
233517	5.02×10^{-01}	$3.60 \times 10^{+00}$	$7.60 \times 10^{+00}$	$5.10 \times 10^{+00}$	9.62×10^{-2}
3003	4.78×10^{-01}	3.21×10^{-01}	4.00×10^{-01}	$1.00 \times 10^{+00}$	8.26×10^{-4}
10476	$2.00 \times 10^{+00}$	6.64×10^{-01}	4.00×10^{-01}	$1.25 \times 10^{+00}$	2.40×10^{-3}
10647	8.22×10^{-01}	3.42×10^{-01}	8.51×10^{-01}	$1.08 \times 10^{+00}$	2.10×10^{-3}
10700	$9.56 \times 10^{+00}$	$2.16 \times 10^{+00}$	5.12×10^{-01}	$1.36 \times 10^{+00}$	2.37×10^{-3}
14055	$1.07 \times 10^{+00}$	4.70×10^{-01}	8.58×10^{-01}	8.48×10^{-01}	4.71×10^{-4}
16157	5.43×10^{-01}	2.01×10^{-01}	4.00×10^{-01}	$1.07 \times 10^{+00}$	1.35×10^{-2}
18978	$1.38 \times 10^{+00}$	3.53×10^{-01}	4.00×10^{-01}	$1.00 \times 10^{+00}$	6.75×10^{-4}
20010	$4.11 \times 10^{+00}$	9.70×10^{-01}	2.87×10^{-01}	$1.00 \times 10^{+00}$	1.65×10^{-3}
22049	$9.52 \times 10^{+00}$	$2.65 \times 10^{+00}$	$1.66 \times 10^{+00}$	$1.89 \times 10^{+00}$	2.46×10^{-3}
38393	$4.60 \times 10^{+00}$	$1.08 \times 10^{+00}$	4.00×10^{-01}	$1.00 \times 10^{+00}$	1.28×10^{-3}
43955	1.47×10^{-01}	1.45×10^{-01}	4.42×10^{-01}	$1.46 \times 10^{+00}$	1.00×10^{-4}
49336	2.39×10^{-01}	1.74×10^{-01}	1.72×10^{-01}	$1.09 \times 10^{+00}$	2.67×10^{-4}
53376	6.86×10^{-01}	2.79×10^{-01}	4.00×10^{-01}	$4.46 \times 10^{+00}$	6.85×10^{-2}
68456	$1.46 \times 10^{+00}$	2.72×10^{-01}	4.00×10^{-01}	$1.85 \times 10^{+00}$	1.42×10^{-3}
69830	9.66×10^{-01}	3.75×10^{-01}	4.00×10^{-01}	$1.00 \times 10^{+00}$	2.80×10^{-3}
71155	$1.15 \times 10^{+00}$	4.49×10^{-01}	4.00×10^{-01}	$1.00 \times 10^{+00}$	4.13×10^{-4}
73390	5.11×10^{-01}	2.50×10^{-01}	5.32×10^{-01}	$1.71 \times 10^{+00}$	2.29×10^{-4}
95418	$4.80 \times 10^{+00}$	$1.39 \times 10^{+00}$	6.27×10^{-01}	$1.00 \times 10^{+00}$	3.85×10^{-4}
108483	5.61×10^{-01}	2.64×10^{-01}	4.00×10^{-01}	$5.20 \times 10^{+00}$	9.83×10^{-5}
114981	1.56×10^{-01}	1.40×10^{-01}	2.16×10^{-01}	7.38×10^{-01}	1.00×10^{-3}
128167	$1.60 \times 10^{+00}$	3.76×10^{-01}	4.00×10^{-01}	$1.00 \times 10^{+00}$	1.12×10^{-3}
139006	$5.92 \times 10^{+00}$	$1.73 \times 10^{+00}$	7.51×10^{-01}	$1.00 \times 10^{+00}$	3.76×10^{-4}
143018	$3.05 \times 10^{+00}$	$5.47 \times 10^{+00}$	$9.25 \times 10^{+00}$	$8.41 \times 10^{+00}$	1.25×10^{-4}
149630	9.64×10^{-01}	2.47×10^{-01}	2.64×10^{-01}	$1.00 \times 10^{+00}$	3.23×10^{-4}
153968	3.68×10^{-01}	3.77×10^{-01}	4.00×10^{-01}	$1.71 \times 10^{+00}$	3.32×10^{-2}
161868	$1.41 \times 10^{+00}$	5.10×10^{-01}	$1.29 \times 10^{+00}$	$2.35 \times 10^{+00}$	4.14×10^{-4}
162917	5.44×10^{-01}	2.50×10^{-01}	3.80×10^{-01}	$1.26 \times 10^{+00}$	1.60×10^{-3}
172167	$4.16 \times 10^{+01}$	$1.10 \times 10^{+01}$	$9.51 \times 10^{+00}$	$7.76 \times 10^{+00}$	3.55×10^{-4}
176638	4.74×10^{-01}	3.95×10^{-01}	4.00×10^{-01}	$1.28 \times 10^{+00}$	5.17×10^{-4}
181296	5.39×10^{-01}	4.77×10^{-01}	5.33×10^{-01}	$1.00 \times 10^{+00}$	7.63×10^{-4}
181869	8.21×10^{-01}	3.48×10^{-01}	4.00×10^{-01}	$1.00 \times 10^{+00}$	3.16×10^{-4}
214953	6.26×10^{-01}	4.43×10^{-01}	4.00×10^{-01}	$1.00 \times 10^{+00}$	3.16×10^{-3}
216956	$1.82 \times 10^{+01}$	$4.81 \times 10^{+00}$	$9.02 \times 10^{+00}$	$1.12 \times 10^{+01}$	6.43×10^{-4}
224392	5.21×10^{-01}	1.93×10^{-01}	4.00×10^{-01}	$1.00 \times 10^{+00}$	8.01×10^{-4}

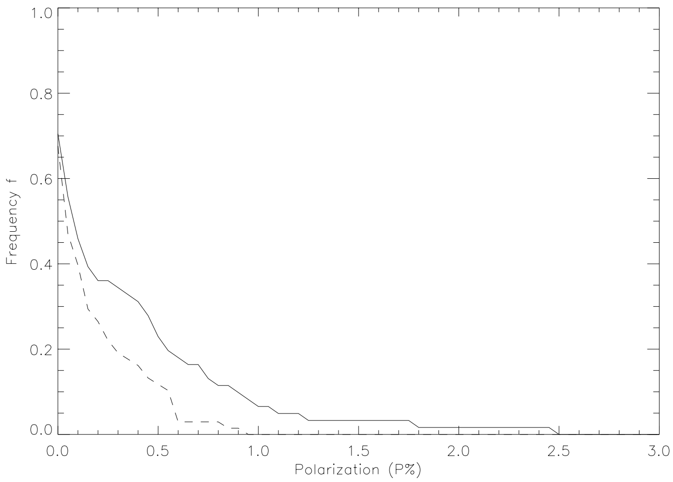

Fig. 2. Frequency distribution of observed polarization values for Vega-like and normal field stars. f is the fractional number of stars with observed polarization larger than a given value. Solid line represents Vega-like stars and dashed line normal field stars

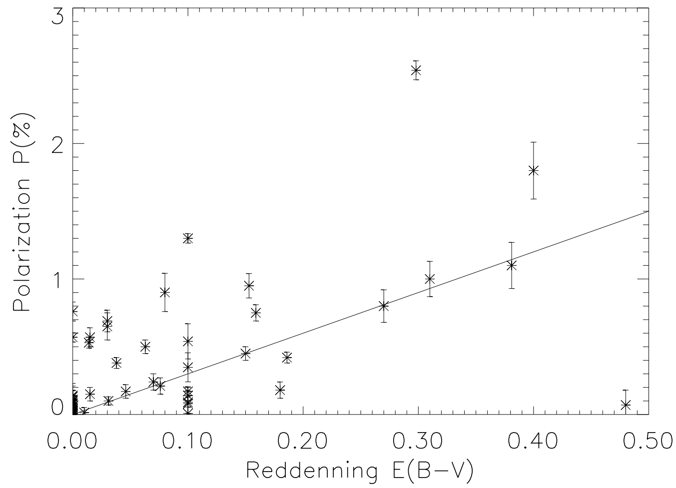

Fig. 3. Percentage polarization against reddenning for Vega-like stars.The average interstellar relation $P(\%)/E(B-V) = 3$ is shown as the solid line

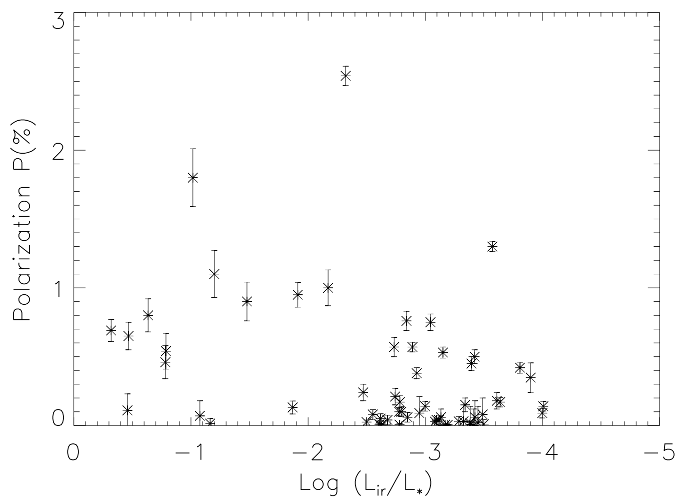

Fig. 4. Plot of percentage polarization against the fractional infrared excess for Vega-like stars

Kolmogorov-Smirnoff test shows that the two samples (Vega-like and normal field stars) are different to 99.7%.

For the Vega-like stars that show relatively large degree of polarization, the observed polarization cannot be accounted for by normal interstellar polarization and must be circumstellar in origin. Circumstellar dust around these stars, to which the observed infrared excesses are ascribed, can cause polarization by the the process of scattering of the light from the central star. In order to be able to produce a net polarization in the integrated light the dust must be distributed in a non-spherical geometry. These non-spherical distributions could be flattened disks around the stars similar to those in β Pic. The disk planes should have relatively small inclinations with the observer's line of sight. Given this constraint on the inclination of the disks, the difference between the Vega-like stars and the normal stars noticed in Fig. 1 becomes even more significant, because only a fraction of the stars with disks will have favourable inclinations.

The large values of polarization observed for Vega-like stars thus support the existence of dusty disks around these stars. The polarization is produced by scattering of light from the central star. In contrast, the interstellar polarization is caused by selective extinction due to nonspherical dust grains aligned by the intertellar magnetic field. The interstellar polarization shows a correlation with reddening given by the average relation: $P_V/E(B-V) = 3\% mag^{-1}$. The circumstellar dust in Vega-like stars is believed to consist of relatively large grains (a few tens of microns (Backman & Parsce 1993)) that are not expected to produce any additional reddening at optical wavelengths. Thus large values of polarization may result even with small values of reddening at small distances. Fig. 3 shows a plot of the observed polarization against reddening $E(B-V)$ for the Vega-like stars, together with the line representing the average relation followed by interstellar polarization and reddening. It can be seen that there are more stars above this line than below it. Also, there is a lack of correlation between polarization and reddening in Vega-like stars for smaller values of reddening. Only at relatively large distances when the interstellar component becomes large does the observed polarization begin to generally increase with reddening.

Circumstellar dust in Vega-like stars absorbs light from the central star and radiates thermally in the infrared. Dust also scatters starlight and produces polarization. One may therefore expect some correlation between the observed polarization in the optical and the excess infrared emission from these objects. In Fig. 4 we plot the observed percentage polarization against the excess infrared luminosity (L_{IR}) as a fraction of the total bolometric luminosity (L_*) of the star (the ratio L_{IR}/L_*) for the Vega-like stars. The infrared excess L_{IR} has been computed from the observed flux densities in the IRAS bands using the equation (Cox 2000)

$$F_{IR}(7-135\,\mu m) = 1.0\times10^{-14}(20.653 f_{12} \\ +7.538 f_{25} + 4.578 f_{60} + 1.762 f_{100}) W m^{-2}$$

for the total infrared flux and the appropriate distance factor $4\pi d^2$ where d is the distance to the star. The stellar bolometric luminosity L_* corresponds to the bolometric luminosity of a normal star of the same spectral type as that of the Vega-like star under consideration. The L_{IR}/L_* values are listed in Table 3. A positive correlation is apparent from Fig. 4. Vega-like stars with relatively larger infrared excesses tend to have larger values of polarization in the optical. The ratio L_{IR}/L_* can be taken to be a rough measure of the dust optical depth τ in the optical where the absorption of starlight takes place. The observed values of the ratio L_{IR}/L_* imply τ in the range $\sim 10^{-4}$ - $\sim 10^{-1}$. For large dust grains (grain size $a \gg \lambda$, the wavelength of light), that are generally thought to dominate the dust disks of Vega-like stars, the absorption and scattering efficiencies can be taken to be ~ 1. If the polarization is produced by scattering of starlight by the same dust that absorbs stellar radiation and emits thermally in the infrared, then for the observed range of the L_{IR}/L_* ratio the expected range of polarization values would be $\sim 10^{-2}\% - \sim 10\%$. Stars with $L_{IR}/L_* \sim 10^{-2}$ would have polarization up to the level of $\sim 1\%$. Here it is assumed that the circumstellar material is optically thin so that there is single scattering only (Bastien 1987). The maximum linear polarization that can be produced in ellipsoidal models with single scattering is about 1.1% (Shawl 1975). Larger values of polarization can result if the direct light from the central star is extincted by obscuring dust in front of the star. Also, the observed polarization depends on the flatness and orientation of the dust disk. It is to be noted from Fig. 4 that several stars with $L_{IR}/L_* \sim 10^{-3}$ or less also show polarization $\sim 0.5\%$, much larger than the expected values $<\sim 0.1\%$. It is possible that these stars have an additional dust component with smaller grains with high albedo. This population of grains would cause relatively large polarization by scattering without producing large infrared excesses.

4. Conclusions

The results of the present study of the polarimetric behaviour of Vega-like stars can be summarized as follows.

- Vega-like stars generally show optical linear polarization that is much larger than that which can be ascribed to interstellar polarization along the line of sight to these relatively nearby objects.
- The anomalous polarization in Vega-like stars is caused by scattering of stellar light due to circumstellar dust distributed in non-spherically symmetric envelopes, and is fully consistent with a distribution in flattened disks.
- The absence of any excess reddening in these stars is consistent with the dust grains in their circumstellar disks being relatively large in size.
- In some Vega-like stars that show relatively small infrared excesses but large values of polarization, an additional component of dust consisting of smaller grains with high albedo may also be present.

Multiwavelength polarization measurements of Vega-like stars would be able to shed more light on the nature and distribution of the dust in their circumstellar environment.

Acknowledgements. We would like to thank the referee Prof. P. F. Bastien for several very useful comments.

References

Aumann H.H., et al., 1984, ApJ 278, L23
Backman D.E., Paresce F., 1993, In: Levy E.H., Lunine J.I. (eds.) Protostars and Planets III, Univ. Arizona Press, Tucson, p. 1253
Bastien P., 1987, ApJ 317, 231
Bastien P., 1988, In: Coyne G.V. (eds.) Polarized Radiation of Circumstellar Origin. Univ. of Arizona Press, Tuscon, p. 541
Coulson I.M., Walther D.M., Dent W.R.F., 1996, In: Holt S.S., Mundy L.G. (eds.) Starformation Near and Far. AIP Conference Proceedings Vol. 393, p. 209
Cox A.N., 2000, Allen's Astrophysical Quantities. 4th edition, Springer-Verlag, New York, p. 154
ESA, 1997, The Hipparcos and Tycho catalogues. ESA SP-1200
Gledhill T.M., Scarrott S.M., Wolstencroft R.D., 1991, MNRAS 252, 50
Heiles C., 2000, AJ 119, 923
Hsu J.C., Breger M., 1982, ApJ 262, 732
Jain S.K., Srinivasulu G., 1991, Opt. Eng. 30, 1415
Jayawardhana R., Fisher S., Hartmann L., et al., 1998, ApJ 503, L79
Kalas P., Jewitt D., 1997, Nat 386, 52
Koerner D.W., Ressler M.E., Werner M.W., Backman D.E., 1998, ApJ 503, L83
Lagrange-Henri A.M., 1995, Ap&SS 223, 19
Malfait K., Bogaert E., Waelkens C., 1998, A&A 331, 211
Mannings V., Barlow M.J., 1998, ApJ 497, 330
Schmidt-Kaler Th., 1965, In: Voigt H.H. (ed.) Landolt-Bornstein. Vol. I of A&A, Group VI, Springer-Verlag, Berlin, p. 298
Serkowski K., 1974, In: Gehrels T. (ed.) Planets Stars and Nebulae studied with photopolarimetry, Univ. Arizona Press, Tucson, p. 135
Shawl S.J., 1975, AJ 80, 602
Skinner C.J., Sylvester R.J., Graham J.R., et al., 1995, ApJ 444, 861
Smith B.A., Terrile R.J., 1984, Sci 226, 142
Vidal-Madjar A., Ferlet R., 1994, In: Ferlet R., Vidal-Madjar A. (eds.) Circumstellar Dust Disks and Planet Formation. Editions Frontieres, Paris, p. 7